Carbohydrate Polymers 234 (2020) 115900

Contents lists available at ScienceDirect

Carbohydrate Polymers

journal homepage: www.elsevier.com/locate/carbpol

Cellulose nanofibers from recycled and virgin wood pulp: A comparative study of fiber development

Shaun Ang, Victoria Haritos, Warren Batchelor*

Bioresource Processing Research Institute of Australia, Department of Chemical Engineering, Monash University, Melbourne, Victoria 3800, Australia

ARTICLE INFO

Keywords:
Recycled fiber
Strength
Reinforcement
Drainage time
SEM
Aspect ratio

ABSTRACT

The global abundance of recycled pulp has introduced opportunities for cellulose nanofiber (CNF) production at lower energy due to the partially fibrillated nature of recycled pulp. This study investigated the potential of recycled pulp as a feedstock for CNF production, comparing recycled bleached de-inked pulp (DIP) predominantly from eucalyptus fibers with virgin bleached eucalyptus kraft (BEK) pulp. The specific energy consumption for CNF production with 10,000 PFI refiner revolutions and 1 homogenization pass was 7 % lower with recycled pulp. At this treatment level, fiber characterization experiments revealed that the CNF from recycled pulp had a median diameter of 19 nm and aspect ratio was 140, similar to that from virgin pulp. The tensile index of unrefined BEK sheets (30 Nm/g) almost doubled (55 Nm/g) when reinforced with only 20 wt% DIP CNF. This work demonstrates that recycled pulp is a viable alternative to virgin pulp feedstocks for CNF production.

1. Introduction

An over reliance on fossil-fuel based plastic packaging has raised numerous issues of unsustainability, continuous increase in raw material prices, recyclability and challenging waste disposal problems (Johansson et al., 2012; Nair, Zhu, Deng, & Ragauskas, 2014). In the fight to reduce our dependency on fossil-fuel materials, cellulose nanofibers (CNF) have been the subject of much research recently. The potential applications of CNF include food packaging, high strength sheets, medical wound dressings, biodegradable films and texturing agents (Klemm et al., 2011; Lavoine, Desloges, Dufresne, & Bras, 2012). CNF are renowned for their excellent optical, thermal, barrier and sheet strength reinforcement potential (Klemm et al., 2011; Zimmermann, Bordeanu, & Strub, 2010), the last of which is the focus of this paper.

CNF can be produced from a wide variety of cellulose materials such as flex, cotton, tunicin, hemp, sugar beet, potato peel, wheat straw and most commonly, wood pulp (Isogai, 2013; Klemm et al., 2011; Lavoine et al., 2012). Surprisingly, very little information exists on the production and properties of CNF made from recovered or recycled wood pulp fibers, compared to more common virgin sources. Some examples of CNF production from recycled pulp fibers include CNF produced from waste newspapers using alkaline treatments and homogenization (Takagi, Nakagaito, & Bistamam, 2013), CNF with high specific surface area produced from recycled thermomechanical newspaper pulp using a supermasscolloider (Josset et al., 2014) and CNF with good reinforcement properties in dissolved cellulose matrixes produced from deinked printing paper using TEMPO oxidation (Hai et al., 2017). It is worth noting that within the context of this research, *virgin* fibers refers to never-dried unrefined pulp fiber. The term *recycled* fibers refers to once-dried sheets which have been soaked and processed in a laboratory or in industry back into pulp.

According to United Nations estimates, the global consumption of paper is currently at 400 million tpa (FAO, 2016). In the global paper industry, recycled pulp fibers are an important substitute for virgin wood pulp as it helps reduce the pressure and impacts of commercial forestry (Bajpai, 2013). The American Forest & Paper Association estimates a national recycled paper recovery rate of 63.5 % in 2010 which is expected to increase to 70 % by 2020 (Bajpai, 2013). The Confederation of European Paper Industries noted that approximately 60 % of all paper and paperboard manufactured in 2010 worldwide is made from recycled pulp fibers (Hubbe, 2014). These trends suggest that further research into abundantly available recycled pulp fibers as a viable feedstock for CNF production is necessary.

The process of recycling once-dried sheets back into pulp causes a decrease in fiber swelling capacity, commonly referred to as hornification (Fernandes Diniz, Gil, & Castro, 2004). This stems from the strong irreversible hydrogen bonds formed with the drying of sheets (Fernandes Diniz et al., 2004). From a morphological perspective, the formation of fiber aggregates with recycled pulp fibers have also been observed due to these strong bonds (Missoum, Bras, & Belgacem, 2012).

* Corresponding author at: 15 Alliance Lane Clayton Campus, Monash University, Victoria 3800, Australia.
E-mail addresses: shaun.ang@monash.edu (S. Ang), victoria.haritos@monash.edu (V. Haritos), warren.batchelor@monash.edu (W. Batchelor).

https://doi.org/10.1016/j.carbpol.2020.115900
Received 15 October 2019; Received in revised form 17 January 2020; Accepted 20 January 2020
Available online 22 January 2020
0144-8617/

Despite this, there are some promising studies with CNF produced from recycled feedstocks. Processing recycled newsprint with a hydrapulper and ultrasonicator resulted in fibers with more than double the specific surface area, improved water absorption values and increase in fiber aspect ratio of 1.28 times over the newsprint pulp (Guo, Jiang, Li, & Li, 2015). Another study produced CNF sheets from never-dried and once-dried bleached softwood and found that the sheet tensile index of the never-dried and once-dried pulps were very similar at about 105 Nm/g (Spence, Venditti, Habibi, Rojas, & Pawlak, 2010). The final average microfibril diameter was observed to be slightly larger at 134 nm with the once-dried pulps, compared to 79 nm with the never-dried pulps (Spence, Venditti, Rojas, Habibi, & Pawlak, 2010). However, the developments in CNF fiber dimensions for both the once-dried and never-dried pulps were not tracked with increasing treatment. A separate study subjected old recycled corrugated containerboard fibers to TEMPO-mediated oxidation and homogenization to produce CNF. The burst index and short-span compressive test index of the containerboard improved by approximately 15 % with the addition of 3 wt% of CNF (Balea et al., 2019). The changes in CNF fiber dimensions with processing were also not tracked.

While these results indicate a promising outlook for CNF produced from recycled feedstocks, uncertainty still exists in how recycled and virgin fiber quality develops for a given amount of mechanical treatment. The ability to tailor CNF dimensions is crucial for applications such as spray coating systems which require very small diameter fibers to prevent nozzle clogging (Shanmugam, Doosthosseini, Varanasi, Garnier, & Batchelor, 2018) and strength reinforcing agents with polymer nanocomposites which depend on the fiber aspect ratio (Kamphunthong, Hornsby, & Sirisinha, 2012).

In this paper, we investigated the potential of recycled pulp fibers as an alternative feedstock to virgin pulp fibers for the production of low diameter and high aspect ratio CNF. CNF reinforced sheets were produced using recycled fiber CNF and their tensile strengths and drainage times were investigated for strength reinforcement applications.

2. Hypotheses

Very low diameter and high aspect ratio CNF can be produced from recycled pulp fibers comparable to that from virgin pulp fibers at lower energy due to the partially fibrillated nature of the recycled pulp fibers. CNF from recycled pulp fibers have great strength reinforcement potential for high strength and fast drainage time CNF reinforced sheet applications.

3. Experimental

3.1. Materials

Recycled bleached de-inked pulp (DIP 0 K) and virgin never-dried unrefined bleached eucalyptus kraft pulp (BEK 0 K) were obtained from Australian Paper. In Australia, all locally produced virgin copy paper is made from BEK. DIP is an industrial recycled pulp fiber source produced from the treatment, repulping and re-bleaching of recovered post-consumer copy paper. BEK was supplied and stored at a low consistency state of about 10 wt% such that it was never-dried. DIP pulp which originates from once-dried paper was also supplied and stored at a low consistency state of about 10 wt%.

A summary of percentage chemical composition of BEK and DIP pulp used for the production of CNF is shown in Table 1. The extractives content was determined using Soxhlet solvent extraction in accordance with the NREL TP-510-42619 analytical protocol method (NREL, 2005). The cellulose and hemicellulose content were determined using the extractive-free biomass method followed by alkaline treatment as reported by (Rowell, 2012). The lignin content was determined using acid hydrolysis in accordance with the ASTM 1721-01 standard test method (ASTM, 2009). The ash content was determined using high temperature combustion in a muffle furnace in accordance with TAPPI T 211 standards (TAPPI, 2002). 3 replicates were performed for each test, with Table 1 summarising the average contents, with their standard deviations obtained.

Table 1
Chemical composition of pulp fibers for CNF production.

Chemical Composition	Average Content (% ± Standard Deviation)	
	BEK (virgin)	DIP (recycled)
Cellulose	78.7 ± 0.8	80.4 ± 0.3
Hemicellulose	17.7 ± 0.4	14.6 ± 0.3
Lignin	3.2 ± 0.1	3.9 ± 0.1
Extractives	0.3 ± 0.1	0.4 ± 0.2
Ash	0.2 ± 0.1	1.6 ± 0.1

3.2. Mechanical refining and high-pressure homogenization for CNF production

PFI mill mechanical refining was performed for both BEK and DIP pulp in accordance with the TAPPI T248 sp-00 standards (TAPPI, 2001a). Both pulps were refined for 10,000, 30,000 and 50,000 revolutions using 24 oven-dry (OD) g of pulp at 10 wt% per batch. After refining, pulps were then homogenized using a GEA Niro Soavi Homogenizer (PANDAPLUS 2000) operating at 1000 bars and 1 wt% consistency. It is worth noting that homogenization was performed immediately after refining such that the refined pulps were not subjected to an intermediate drying stage. The 10,000 and 30,000 refined pulp suspensions were homogenized for 1 pass (10 K1P and 30 K1P) while the 50,000 refined pulp suspension was homogenized for 3 passes (50 K3P). 50 K3P was chosen as the extreme case in order to produce a very fine CNF sample. Here, 50 K3P was set as the upper limit of mechanical energy consumption (upwards of 35,000 kW h/OD t), beyond which the energy demands of CNF production were deemed to be unattractive. The chosen data set of 14 samples (7 for BEK and 7 for DIP) allows for the comparison of a broad range of samples with different fiber qualities.

A Hager EC350 Three-Phase kWh-meter was used to measure the mechanical energy consumption for PFI refining and high-pressure homogenization for all BEK and DIP samples. For the batch PFI refiner, the energy measurements in kWh were normalized by the oven dried fiber mass to obtain values in kWh/OD t fiber. For the continuous homogenizer, the energy measurements in kWh were normalized by suspension mass and concentration to obtain values in kWh/OD t fiber. To check for repeatability, the energy consumption was measured twice for each sample. Table 2 lists a summary of BEK and DIP sample naming conventions, treatment types and energy consumption.

Table 2
Naming conventions for BEK and DIP samples and specific energy consumption.

BEK (virgin) and DIP (recycled) Samples	PFI Mill Refining Revolutions	Homogenization Passes at 1000 bar	Specific Energy Consumption (kWh/OD tonne fiber)	
			BEK	DIP
0 K	0	0	0	0
10 K	10,000	0	3500	3600
30 K	30,000	0	10,600	10,700
50 K	50,000	0	17,700	18,000
10 K1P	10,000	1	10,700	10,000
30 K1P	30,000	1	17,800	16,900
50 K3P	50,000	3	39,300	36,600

3.3. SEM imaging and diameter distribution

For each sample, a drop of 0.001 wt% fiber suspension was cast on a silicon chip and air dried. Each sample was then sputter-coated with iridium for SEM imaging. The samples were observed under a FEI Magellan 400 XHR FEGSEM. The operating parameters of the SEM were set at a 3.0 kV spot size and 6.3 pA current. SEM imaging was performed for all 14 BEK and DIP samples.

Following the same methodology used by (Ang, Haritos, & Batchelor, 2019; Zhang, Batchelor, Varanasi, Tsuzuki, & Wang, 2012) an SEM image was first taken at a low magnification of 175× (400 μm scale bar) to capture the larger pulp fibers for each sample. This low magnification image was divided into 4 quadrants. A high magnification 60,000× (1 μm scale bar) image was taken at each quadrant to capture the smaller CNF. This was done to account for the heterogeneous nature of the sample with both larger pulp fiber bundles and smaller fibrillated CNF. Image J processing software was used to manually measure all fibers in each SEM image. To do this, image pixels were correlated to a pre-determined length scale.

From the literature, a separate study reported a similar method for the determination of CNF length and width using FE-SEM images and ImageJ (Le Van, 2017). In that study, the authors obtained FE-SEM images of softwood CNF fibers at low magnification and at high magnification for the measurement of fiber lengths and widths, respectively. However, only 30 individual fibers were randomly chosen and measured across multiple images (Le Van, 2017).

This is different to our study, where all observable fibers in each SEM image were measured to avoid bias in selecting the fibers. More than 30,000 CNF and pulp fibers were measured in total across the all 14 BEK and DIP samples. CNF from the high magnification images were sorted into histograms with 10 nm and 2 nm sized bins while the pulp fibers from the low magnification images were sorted into histograms with 2000 nm sized bins using OriginPro 8 software. The area of each SEM image was measured and used to calculate the counts/m^2 for each sample. All calculations were performed using the value of the bin center. The full set of DIP SEM images before and after image analysis is located in the Supplementary information (Figs. A.1–A.35). SEM images and diameter distributions of the BEK CNF and pulp fiber were previously reported in (Ang et al., 2019).

3.4. Aspect ratio estimation

Gel point sedimentation experiments were performed for each sample using a series of 250 ml fiber suspensions with solids concentrations between 0.1 wt% and 0.005 wt%. These suspensions were poured into measuring cylinders after thorough mixing with a Kambrook Model KSB7 hand stirrer. Measurements of the initial sediment heights were (h_o) taken and the suspensions were left to settle for more than 2 days. After settling, the final suspension heights (h_s) were then measured. The initial solids concentration (C_o) was plotted as a function of the ratio of final sediment height to initial sediment height (h_s/h_o). Detailed information on this method can be found at (Varanasi, He, & Batchelor, 2013). MATLAB was used to fit smoothing splines (CSAPS function) to the data set with a smoothing spline parameter, p of 0.9998. The gel point of the sample is equivalent to the constant y-intercept value at the origin of the first derivative (Raj et al., 2016).

The aspect ratio of all BEK and DIP samples was estimated using EMT theory from the gel point values (Varanasi et al., 2013). The aspect ratio was estimated using the equation $A = 3.19\, C_c^{-0.58}$ where A is the aspect ratio of the fibers and C_c is the solids concentration of the suspension at the gel point. The equation assumes a cellulose skeletal density of 1500 kg/m^3 (Varanasi et al., 2013).

3.5. Surface charge measurements

The zeta potential of all BEK and DIP samples were measured using a Nanobrook Omni (Brookhaven Instruments). Measurements were performed using 0.01 wt% suspensions in a cuvette cell at 25 °C. The zeta potential of each suspension was determined by measuring its electrophoretic mobility from laser Doppler velocimetry and applying it to the Smoluchowski equation using the provided software (Raj, Varanasi, Batchelor, & Garnier, 2015). For each sample, the experiment was repeated using 3 cuvette cells. 10 measurements were performed for each cuvette cell.

3.6. Sheet making and drainage time measurements

60 gsm pure sheets of BEK and DIP were produced with 0.2 wt% pulp suspensions using an Automatic British Handsheet Maker (diameter of 0.159 m). Sheets were formed on GE Whatman 541 Hardened Ashless filter ash paper (22 μm pore sized) fitted on top of a standard 150-size mesh (104 μm pore size). The combination of both filter and standard mesh was chosen to ensure near 100 % retention of pulp and CNF. This allowed for a fair comparison of sheet drainage times for fixed 60 gsm sheets made from various CNF and pulp fiber suspensions with varying degrees of fiber quality. The drainage times of the sheet were measured from when the suspension was first poured into the machine until a completely opaque sheet was observed. 3 replicates were formed for each sample listed in Table 2.

60 gsm CNF reinforced sheets of BEK 0 K reinforced with refined DIP 10 K (5 wt%, 10 wt%, 20 wt% loading) and homogenized DIP 10 K1P (5 wt%, 10 wt%, 20 wt% loading) were also produced. The final grammage of each CNF reinforced sheet was held at 60 gsm. 3 replicates were formed for each CNF reinforced sheet sample and their drainage times measured.

3.7. CNF reinforced sheet strength measurements

All CNF reinforced sheets were conditioned at 23 °C and 50 % RH for 24 h in accordance with TAPPI T402 standards (TAPPI, 2001b). An L&W Micrometer was used to measure the thickness of each sheet at 10 random points. The sheets were cut into 10 cm long strips using a hydraulic press template. An Instron Model 5566 Universal Testing Machine was used to measure the stress-strain load measurements for all strips (TAPPI, 2001c). The strips were then collected, and oven dried to determine the oven dried mass and grammage. More than 20 separate 10 cm strips from 3 replicate sheets were evaluated for each sample.

4. Results and discussion

4.1. Specific energy consumption

The specific energy consumption values for all BEK and DIP samples are summarized in Table 2 below. The energy consumption values for BEK were previously reported in (Ang et al., 2019). Interestingly, the specific energy consumption for PFI refining was only slightly higher with DIP compared to BEK 3600 kW h/OD tonne fiber for DIP 0 K to DIP 10 K and 3500 kW h/OD tonne fiber for BEK 0 K to BEK 10 K. This is consistent with once-dried pulps being slightly more difficult to refine due to the more compact and collapsed structures from hydrogen bonding (Spence, Venditti, Habibi et al., 2010).

Interestingly, the specific energy consumption measured with DIP 10 K1P (10,000 kW h/OD tonne fiber) was 7 % lower compared to BEK 10 K1P (10,700 kW h/OD tonne fiber) for a single pass through this homogenizer operating at 1000 bars for a 1 wt% consistency suspension. This could be attributed to the already partially fibrillated nature of the DIP pulp fibers from the recycling process, evidenced by SEM images shown in Fig. 1. It is believed that the extensive amounts of mechanical fibrillation with refining damaged the irreversible hydrogen bonds and shortened the fiber lengths with once-dried pulps (Spence, Venditti, Habibi et al., 2010).

The energy consumption values had only slight variations with

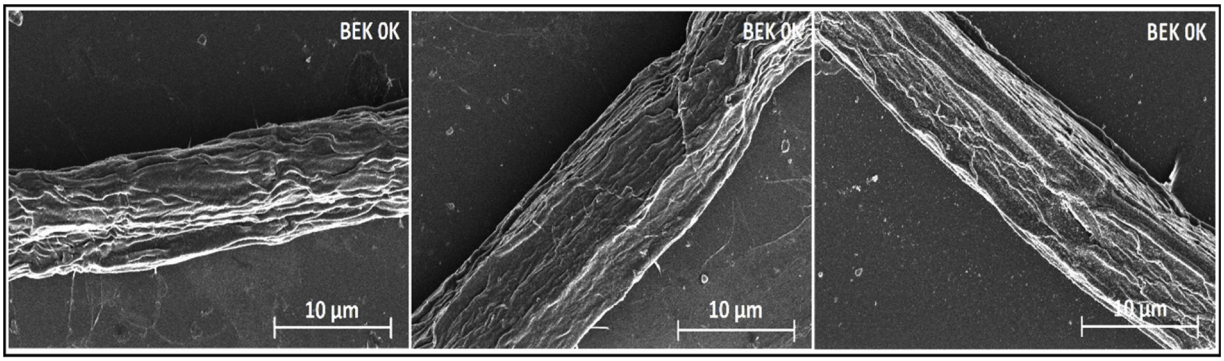

(a)

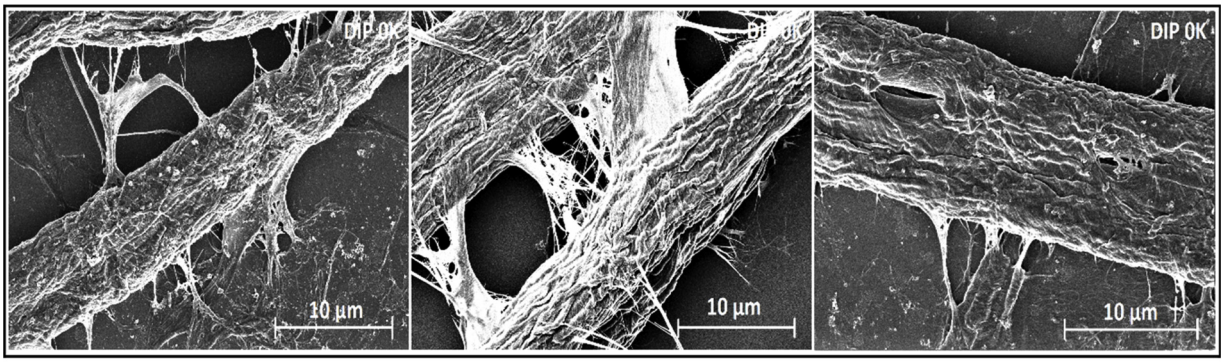

(b)

Fig. 1. SEM images of unrefined **(a)** BEK 0 K and **(b)** DIP 0 K pulp fibers.

6400 kW h/OD tonne fiber for the case of DIP 10 K to DIP 10 K1P and 6200 kW h/OD tonne fiber for all other cases DIP 30 K to DIP 30 K1P, DIP 50 K to DIP 50 K1P, DIP 50 K1P to DIP 50 K2P and DIP 50 K2P to DIP 50 K3P. Energy consumption values for the repeated batch were consistent with the first batch within a 3–6 % error between 6400–6800 kW h/OD tonne fiber. Here, DIP pulp fibers are shown to have great potential as a lower energy solution for CNF production with homogenization.

4.2. SEM imaging

SEM images of unrefined pulp fibers (BEK 0 K and DIP 0 K) and refined and homogenized CNF (BEK 10 K1P and DIP 10 K1P) are shown in Figs. 1 and 2 respectively. From Fig. 1a, the BEK 0 K pulp fiber wall structure is shown to be intact and exhibits very little signs of fibrillation. In contrast, the DIP 0 K pulp fibers in Fig. 1b exhibit many signs of shearing and fiber fibrillation due to the recycling process. The comprehensive set of SEM images for all DIP 0 K, 10 K, 30 K, 50 K, 10 K1P, 30 K1P and 50 K3P samples can be found in the Supplementary information (Figs. A.1–A.35). The comprehensive set of SEM images for all BEK 0 K, 10 K, 30 K, 50 K, 10 K1P, 30 K1P and 50 K3P samples were published in our previous work located in (Ang et al., 2019).

4.3. Diameter distribution

The CNF fiber diameters of BEK and DIP 10 K, 10 K1P and 50 K3P were sorted into histograms with 10 nm and 2 nm sized bins in Fig. 3. As shown in Fig. 3a and b, the heavily refined BEK 10 K and DIP 10 K had similar peak frequency bin centers diameters of about 10 – 20 nm. From Fig. 3c and d, homogenization was shown to greatly increase the total number of fibers per unit area as evidenced by the increase in peak heights of 10 K1P over 10 K sample. Here, both BEK 10 K1P and DIP 10 K1P had similar peaks of 15 nm and normalized fiber counts per unit area. The differences in fiber fibrillation between BEK and DIP samples become more noticeable after 3 homogenization passes, with the peak frequency occurring at the 9 nm and 13 nm bin for BEK 50 K3P and DIP 50 K3P respectively, as shown in Fig. 3f.

Results from statistical analysis of BEK and DIP CNF and pulp fiber diameter distribution are shown in Table A.1 found in the supplementary material. This table compares both samples for a given amount of treatment. The results for BEK were previously published in (Ang et al., 2019). From Table A.1, most fiber distributions had very large positive skewness and kurtosis values showing a long right tail-end distribution with a sharp peak. Skewness is a measure of the asymmetry of a distribution from that of a normal distribution, with a normal distribution having a skewness value of zero. Kurtosis is a measure of how much the tail-ends of a distribution differ from the tail-ends of a normal distribution, with a higher kurtosis value representing a sharp peak in the data set. In this study, the asymmetrical distribution obtained is consistent with sample heterogeneity (few larger sized pulp fibers and extremely high number of CNF fibers) shown in Fig. 2. Because of this, median fiber diameter was chosen as the best measure of central tendency to describe the trends observed and these medians are given in Table 3.

From the pulp fiber measurements in Table A.1, the unrefined DIP 0 K median pulp fiber diameter was 12 % smaller than that of BEK. This is consistent with the DIP pulp fibers being partially fibrillated from repulping and reprocessing. At the highest level of mechanical processing, both samples had similar median pulp fiber diameters of 2.8 µm and 2.6 µm for DIP 50 K3P and BEK 50 K3P respectively, although the fiber counts for the DIP pulp fibers were notably higher than that of the BEK pulp fibers indicating that less of the DIP pulp fibers had been fibrillated into CNF during processing. This could be attributed to the hornified state and strong irreversible hydrogen bond crosslinks formed between the recycled fibers (Fernandes Diniz et al., 2004; Spence, Venditti, Rojas et al., 2010) which reduces the fibrillation efficiency.

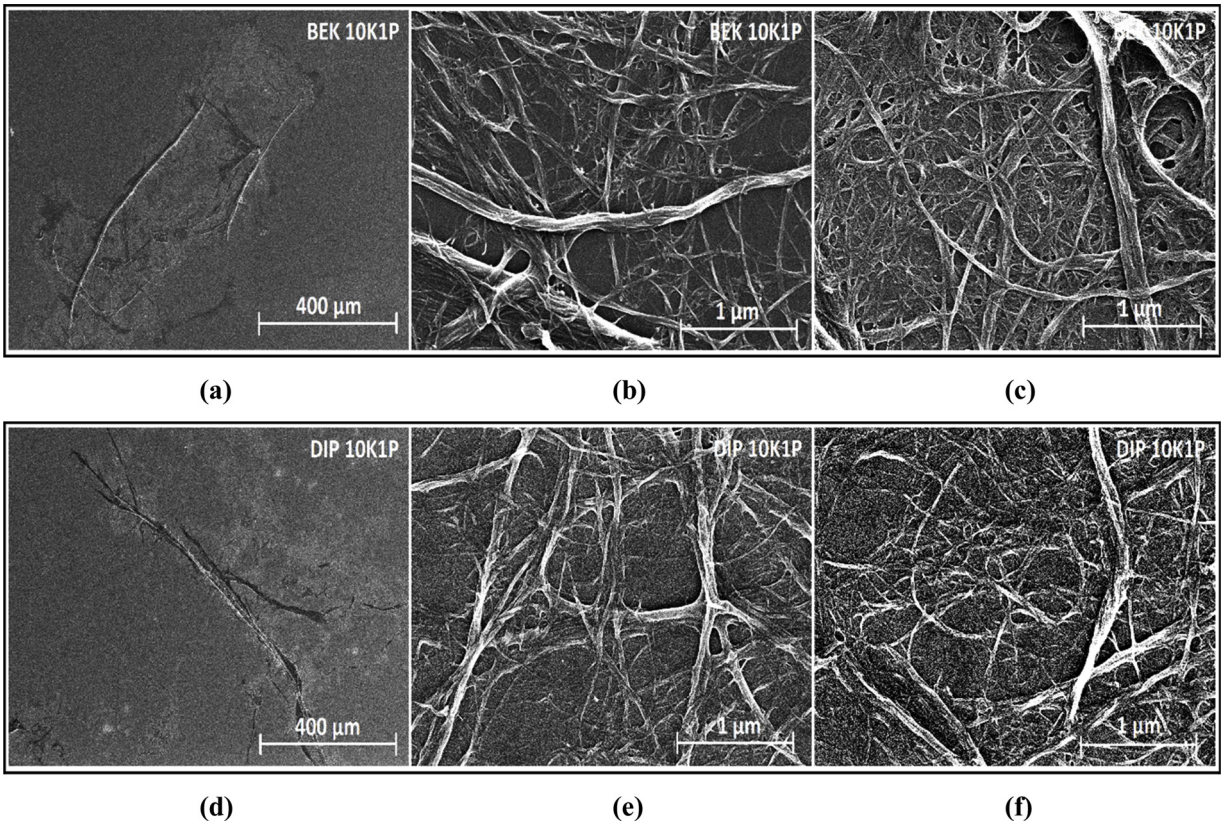

Fig. 2. SEM images of BEK 10 K1P at **(a)** low magnification and **(b) (c)** high magnification and DIP 10 K1P at **(d)** low magnification and **(e) (f)** high magnification.

From the CNF measurements in Table A.1, both BEK and DIP had similar median CNF fiber diameters of approximately 31 nm and 34 nm respectively after 10,000 PFI revolutions. One high-pressure homogenization pass reduced the median CNF fiber diameter by 44 % and 45 % for DIP and BEK, respectively. Interestingly, increasing the number of homogenization passes had a more prominent effect with further decreasing the median CNF fiber diameter of BEK (12 nm for BEK 50 K3P) compared to DIP (18 nm for DIP 50 K3P). In both cases however, the frequency of fiber counts per unit area increased.

4.4. Aspect ratio estimation

The gel point sedimentation experiments (Fig. 4) show that increasing refining and homogenization reduces the gel point, as evidenced by the decreasing slope. The gel point is the lowest solids concentration at which fibers form a continuous network (Varanasi et al., 2013). Aspect ratio estimated from gel points using Effective Median Theory are shown in Table 3. Unrefined DIP 0 K had a slightly higher aspect ratio of 92 over unrefined BEK 0 K of 84. Both BEK and DIP had similar aspect ratios, except at the highest levels of mechanical treatment. Indicative fiber lengths calculated from median diameter and aspect ratio are given in Table A.2 in the Supplementary information.

4.5. Surface charge measurements

Zeta potential results obtained were plotted against the inverse of median CNF diameter in Fig. 5. The inverse of median CNF diameter from the high magnification SEM images will be proportional to the fiber specific surface area. The results with BEK and DIP are consistent with the literature, which shows that increasing the amount of mechanical treatments increases the fiber surface charge due to progressive fiber fibrillation (Dimic-Misic, Maloney, & Gane, 2018). Results show that the average zeta potential of unrefined DIP 0 K of -13.5 mV was slightly lower than BEK 0 K at -11.0 mV. This is again consistent with the partially fibrillated nature of the DIP pulp fibers which results in a higher overall charge. All refined DIP samples had approximately similar zeta potential values of -18 ± 2 mV while all refined BEK samples had slightly lower zeta potential values of -22 ± 3 mV. This again could be attributed to the strong hydrogen bonds with recycled fibers which reduces their surface accessibility with more fibers being coalescent (Fernandes Diniz et al., 2004). Interestingly, 50 K3P treatments decreased the zeta potential of both BEK and DIP suspensions to similar values of approximately -30 mV. Both sets of samples could be fitted with a single straight line, suggesting that there is one overall value of charge per unit area. Here, the results also indicate that there is no observable difference in the surface chemistry of BEK and DIP since both data sets could be fitted with a single straight line. This is consistent with the composition values presented in Table 1, where both BEK and DIP were shown to be similar in terms chemical composition.

4.6. Pure sheet and CNF reinforced sheet drainage time

The drainage times for the 60 gsm pure sheets of BEK and DIP were plotted as a function of median diameter in Fig. 6. The median diameter was taken from the CNF measurements obtained using the high magnification SEM images, believed to control the sheet drainage times. This median CNF fiber diameter will be very similar to that of the whole sample, given the significantly higher CNF to wood pulp fiber counts.

From Fig. 6, the DIP sheets typically took less than half the time to drain than the BEK sheets, at the same level of mechanical treatment. This is attributed to the smaller median CNF fiber diameters of the BEK over the DIP for a given amount of mechanical treatment. These results are consistent with flow velocity described in the Kozeny-Carman equation (Carman, 1937) whereby the smaller the particle diameter,

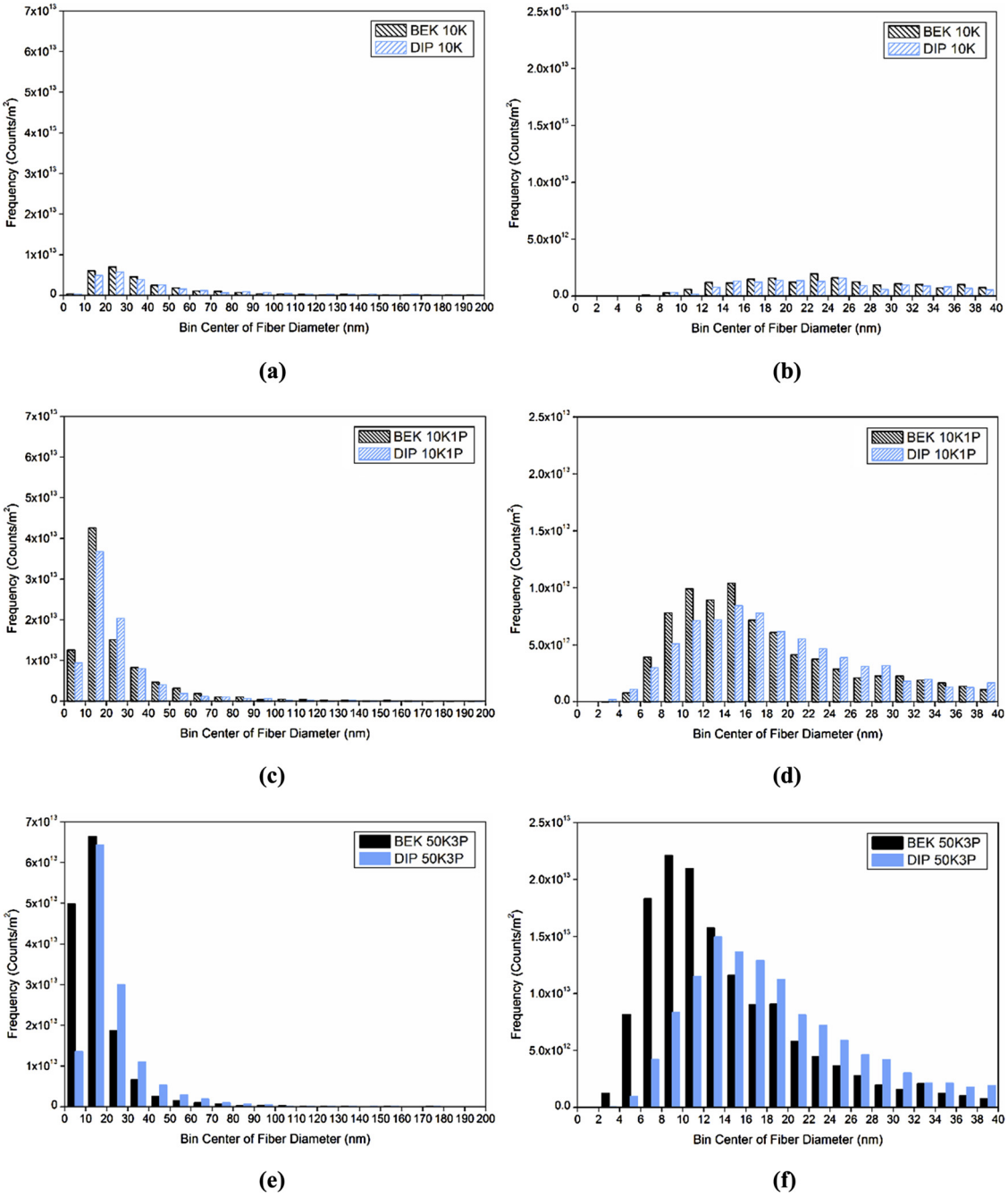

Fig. 3. BEK and DIP diameter distribution of 10 K CNF sorted into **(a)** 10 nm and **(b)** 2 nm bin sizes, 10 K1P CNF sorted into **(c)** 10 nm and **(d)** 2 nm bin sizes, 50 K3P CNF sorted into **(e)** 10 nm and **(f)** 2 nm bin sizes.

the smaller the superficial flow velocity of fluid flowing through a packed bed. From the literature, recycled fibers are also believed to be stiffer which forms a bulkier and more porous mat to reduce drainage times (Hubbe & Heitmann, 2007). It is worth noting however that the drainage times reported here in minutes are still orders of magnitude larger than what is common with conventional papermaking processes. As such, CNF reinforced sheets were formed with the aim of reducing the drainage times to seconds while still producing a high strength sheet.

The drainage times of the CNF reinforced sheets produced were plotted as a function of weighted specific energy consumption as shown in Fig. 7. As shown in Fig. 7, even at the highest CNF reinforcement level of 20 wt% DIP 10 K1P, the drainage times of these reinforced sheets were less than 1 min.

4.7. CNF reinforced sheets sheet strength

Fig. 8a and b show the tensile index of the CNF reinforced sheets as a function of percentage of refined and homogenized fibers added, and weighted specific energy consumption, respectively. The tensile index of pure BEK 10 K and BEK 10 K1P were previously published in (Ang et al., 2019). Here, a straight line connecting BEK 0 K to BEK 10 K and BEK 10 K1P was drawn to guide the reader. It is worth noting that this trendline does not make any definitive conclusions about the linear developments in tensile index for pure BEK in the absence of a refining curve. This was merely done to ease the comparison between the experimental data points in this study. From Fig. 8a, the unrefined BEK 0 K sheet tensile index of approximately 30 Nm/g was shown to increase by almost two-fold to 55 Nm/g with only a 20 wt%

Table 3
Gel point, aspect ratio and fiber length estimation of BEK and DIP samples.

Degree of Treatment	Gel Point, C_c (wt %)		EMT Aspect Ratio, A		Median Diameter, d			
					CNF (nm) (High Mag. Images)		Pulp Fiber (μm) (Low Mag. Images)	
Sample	BEK	DIP	BEK	DIP	BEK	DIP	BEK	DIP
0 K	0.353	0.304	84	92	13,113	126	14.5	12.8
10 K	0.256	0.278	102	97	31	34	12.2	7.7
30 K	0.243	0.270	105	98	25	27	11.3	6.1
50 K	0.230	0.246	108	104	24	26	8.9	4.9
10 K1P	0.144	0.147	142	140	17	19	2.4	3.5
30 K1P	0.089	0.109	188	167	16	19	2.9	2.5
50 K3P	0.063	0.085	229	193	12	18	2.8	2.6

reinforcement with recycled DIP 10 K1P. Interestingly, all sheets reinforced with DIP 10 K1P performed better in sheet tensile index compared to the trendline of BEK 0 K to pure BEK 10 K1P, at a given percentage of refined and homogenized fiber added. For example, a CNF reinforced BEK sheet reinforced with 20 wt% DIP 10 K1P had an average tensile index value of 55 Nm/g which is 17 % higher than the predicted trendline value of approximately 47 Nm/g. This shows that there are synergies from using CNF produced from recycled DIP to reinforce unrefined BEK pulp fibers. These results are also consistent with studies which have demonstrated that the addition of 10%–20% NFC produced from a supermasscolloider to unrefined hardwood sheets resulted in synergistic effects (Hai & Seo, 2018). In that study, the NFC reinforced sheet had a higher sheet tensile index compared to that of a pure non-reinforced refined hardwood sheet at the same density. This was attributed to the formation of more inter-fiber bonds with the NFC reinforced sheet (Hai & Seo, 2018).

When comparing to weighted specific energy consumption in Fig. 8b, the sheets reinforced with 20 wt% DIP 10 K1P required approximately 2000 kW h/OD tonne fiber for an average tensile index of 55 Nm/g. This energy value is notably lower compared to the expected trendline value of pure BEK 0 K to pure BEK 10 K1P, which for a predicted tensile index of 55 Nm/g would require about 50 % more energy at approximately 3000 kW h/OD tonne fiber. Here most importantly, we have demonstrated that CNF produced from DIP pulp fibers can be made at lower energy and have great potential as a reinforcement material to produce high strength sheets.

Fig. 8c shows the correlation between sheet drainage time and tensile index for all samples. As shown in Fig. 8c, high strength CNF reinforced sheets are shown to be achievable at reasonably low drainage times. CNF will increase the bonding between pulp fibers as well as forming its own network.

These results were generally consistent with literature data. In one study, the addition of 10 wt% commercial CNF resulted in a 35 % increase in bleached hardwood sheet tensile index (Madani, Kiiskinen, Olson, & Martinez, 2011). In our study, the addition of 10 wt% DIP

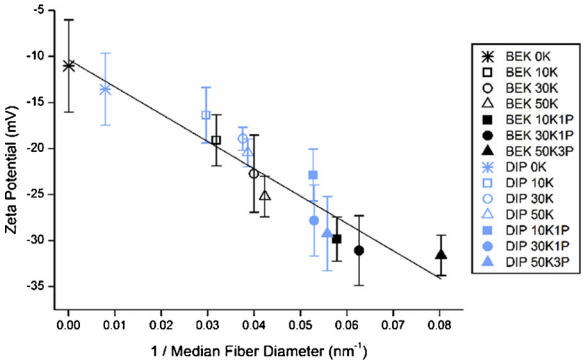

Fig. 5. Zeta potential measurements for BEK and DIP samples with standard deviation error bars.

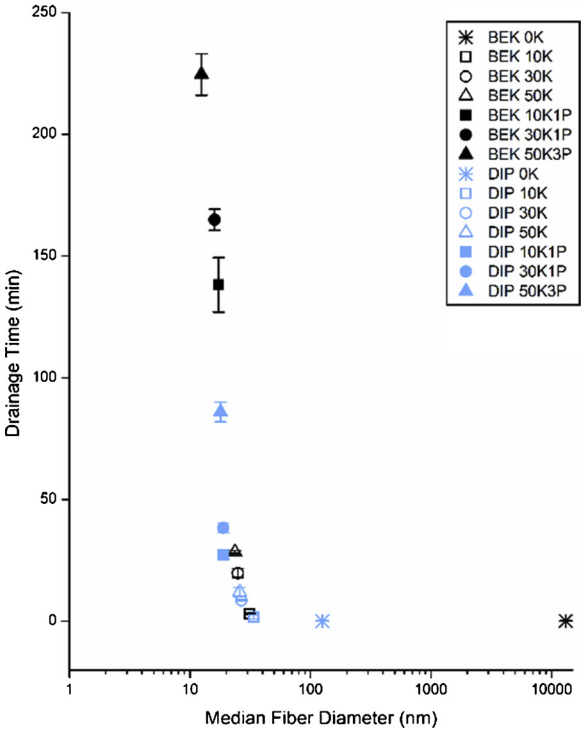

Fig. 6. Sheet drainage times for pure sheets of BEK and DIP with standard deviation error bars.

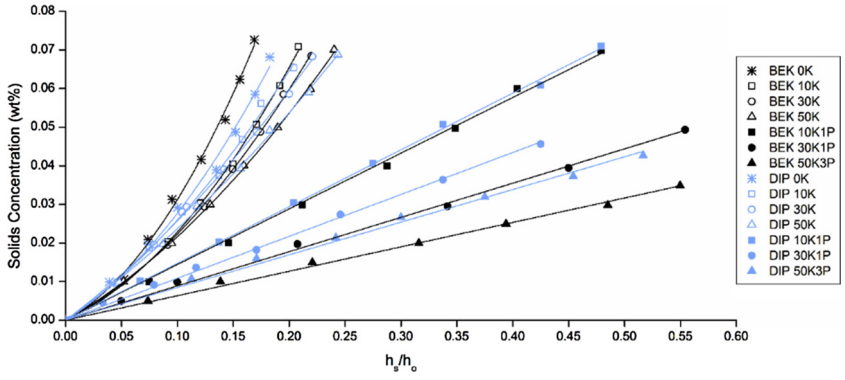

Fig. 4. Sedimentation behaviour of all BEK and DIP samples.

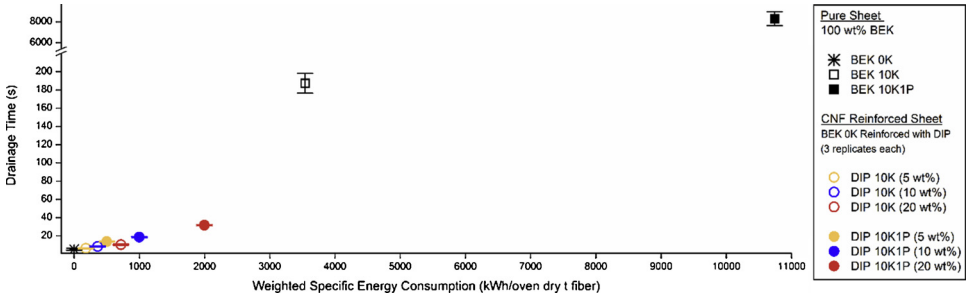

Fig. 7. Drainage time of CNF reinforced sheets with standard deviation error bars as a function of weighted specific energy consumption with 95 % confidence interval error bars.

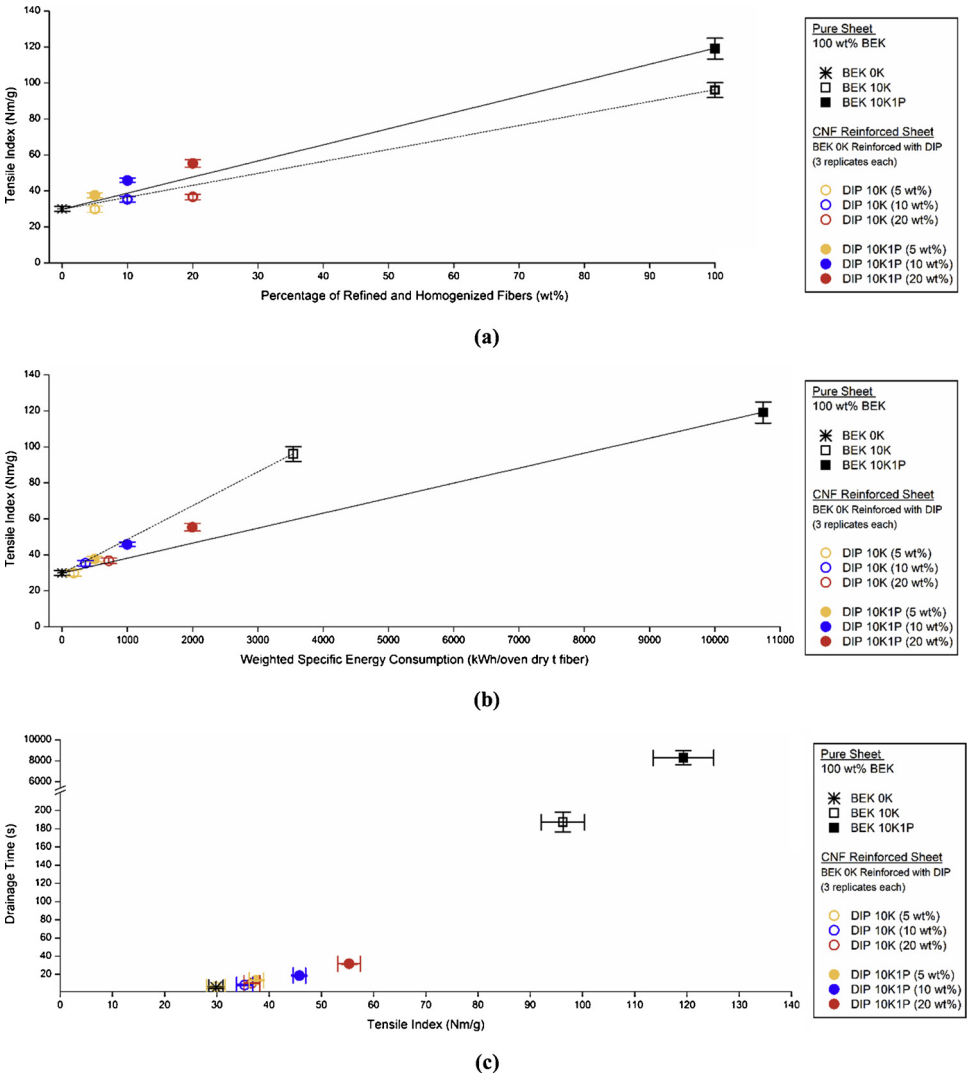

Fig. 8. Tensile index of CNF reinforced sheets as a function of **(a)** percentage of refined and homogenized fibers **(b)** weighted specific energy consumption and **(c)** drainage time with 95 % confidence interval error bars.

10 K1P CNF was shown to result in an approximate 50 % increase in sheet tensile index from 30 Nm/g with pure BEK 0 K sheets to 45 Nm/g with the CNF reinforced sheets shown in Fig. 8b. In another study, the addition of 4 wt% CNF resulted in about a 20 % increase in sheet tensile index from 40 Nm/g to 48 Nm/g (Eriksen, Syverud, & Gregersen, 2008), similar to the 26 % increase observed with 5 wt% DIP 10 K1P CNF addition that was observed here.

Here, we have demonstrated that high strength CNF reinforced sheets can be produced at lower drainage times with CNF produced from recycled fibers. This confirms that CNF from recycled fibers have excellent potential as a reinforcement agent.

5. Conclusion

The results here showed that recycled pulp is an extremely viable source for very low diameter CNF production, with fiber diameters comparable to that of the virgin pulp but requiring 7 % less energy to produce. Fiber characterization experiments revealed that DIP CNF had

a median fiber diameter of 34 nm after the 10 K treatment and 19 nm after the 10 K1P treatment, similar to that of BEK CNF at the same level of treatment. With fiber aspect ratio, the initial unrefined DIP pulp fiber aspect ratio at 92 increased to 97 after the 10 K treatment and 140 after the 10 K1P treatment, also similar to that of BEK at the same level of treatment. Pure CNF sheets from DIP were shown to consistently drain quicker compared to those made from BEK. However, all pure CNF sheets had drainage times measured in minutes, such as BEK 10 K1P at 138 min and DIP 10 K1P at 27 min. Critically, the CNF from DIP provided excellent strength when used as a reinforcing fiber in sheetmaking, while keeping the drainage time low. The addition of 20 wt% DIP 10 K1P into unrefined BEK sheets almost doubled the sheet tensile index from 30 Nm/g to 55 Nm/g. Most importantly, even the most heavily DIP CNF reinforced sheets had drainage times measured in seconds.

In the push towards producing materials which are sustainable, renewable and recyclable, this study demonstrates that recycled fibers should be strongly considered as a feedstock for CNF production and are worth researching further.

CRediT authorship contribution statement

Shaun Ang: Conceptualization, Methodology, Investigation, Formal analysis, Writing - original draft, Writing - review & editing. **Victoria Haritos:** Writing - review & editing, Supervision. **Warren Batchelor:** Conceptualization, Writing - review & editing, Supervision, Project administration, Funding acquisition.

Acknowledgements

The authors wish to thank Australian Paper Maryvale for their ongoing support with the project. The authors wish to acknowledge the Monash Centre of Electron Microscopy (MCEM) for use of their SEM facilities. The authors also wish to thank Debjani Ghosh for her help with the chemical composition of pulps. Shaun Ang would like to thank the Australian Government for a Research Training Program scholarship.

Appendix A. Supplementary data

Supplementary material related to this article can be found, in the online version, at doi:https://doi.org/10.1016/j.carbpol.2020.115900.

References

Ang, S., Haritos, V., & Batchelor, W. (2019). Effect of refining and homogenization on nanocellulose fiber development, sheet strength and energy consumption. *Cellulose, 26*(8), 4767–4786.

ASTM (2009). *ASTM 1721-01 standard test method for the determination of acid-insoluble residue in biomass.* West Conshohocken, Pennsylvania, United States: American Society for Testing and Materials.

Bajpai, P. (2013). *Recycling and deinking of recovered paper.* London: Elsevier.

Balea, A., Sanchez-Salvador, J. L., Monte, M. C., Merayo, N., Negro, C., & Blanco, A. (2019). In situ production and application of cellulose nanofibers to improve recycled paper production. *Molecules, 24*(9), 1800–1813.

Carman, P. C. (1937). Fluid flow through granular beds. *Transactions of the Institution of Chemical Engineers, 15*, 150–166.

Dimic-Misic, K., Maloney, T., & Gane, P. (2018). Effect of fibril length, aspect ratio and surface charge on ultralow shear-induced structuring in micro and nanofibrillated cellulose aqueous suspensions. *Cellulose, 25*(1), 117–136.

Eriksen, Ø., Syverud, K., & Gregersen, Ø. (2008). The use of microfibrillated cellulose produced from kraft pulp as strength enhancer in TMP paper. *Nordic Pulp and Paper Research Journal, 23*(3), 299–304.

FAO (2016). *Food and Agricultural Organization (FAO) of the United Nations 2016 yearbook of forest products.* Rome: FAO Statistics.

Fernandes Diniz, J. M. B., Gil, M. H., & Castro, J. A. A. M. (2004). Hornification—Its origin and interpretation in wood pulps. *Wood Science and Technology, 37*(6), 489–494.

Guo, X., Jiang, Z., Li, H., & Li, W. (2015). Production of recycled cellulose fibers from waste paper via ultrasonic wave processing. *Journal of Applied Polymer Science, 132*(19), 41962–41981.

Hai, L. V., & Seo, Y. B. (2018). Properties of nanofibrillated cellulose prepared by mechanical means. *Cellulose Chemistry & Technology, 52*(9–10), 741–747.

Hai, L. V., Kim, H. C., Kafy, A., Zhai, L., Kim, J. W., & Kim, J. (2017). Green all-cellulose nanocomposites made with cellulose nanofibers reinforced in dissolved cellulose matrix without heat treatment. *Cellulose, 24*(8), 3301–3311.

Hubbe, M. A. (2014). Recycling paper recycling. *BioResources, 9*(2), 1828–1829.

Hubbe, M. A., & Heitmann, J. A. (2007). Review of factors affecting the release of water from cellulosic fibers during paper manufacture. *BioResources, 2*(3), 500–533.

Isogai, A. (2013). Wood nanocelluloses: Fundamentals and applications as new bio-based nanomaterials. *Journal of Wood Science, 59*(6), 449–459.

Johansson, C., Bras, J., Mondragon, I., Nechita, P., Plackett, D., Šimon, P., et al. (2012). Renewable fibers and bio-based materials for packaging applications—A review of recent developments. *BioResources, 7*(2), 2506–2552.

Josset, S., Orsolini, P., Siqueira, G., Tejado, A., Tingaut, P., & Zimmermann, T. (2014). Energy consumption of the nanofibrillation of bleached pulp, wheat straw and recycled newspaper through a grinding process. *Nordic Pulp and Paper Research Journal, 29*(1), 167–175.

Kamphunthong, W., Hornsby, P., & Sirisinha, K. (2012). Isolation of cellulose nanofibers from para rubberwood and their reinforcing effect in poly(vinyl alcohol) composites. *Journal of Applied Polymer Science, 125*(2), 1642–1651.

Klemm, D., Kramer, F., Moritz, S., Lindström, T., Ankerfors, M., Gray, D., et al. (2011). Nanocelluloses: A new family of nature-based materials. *Angewandte Chemie - International Edition, 50*(24), 5438–5466.

Lavoine, N., Desloges, I., Dufresne, A., & Bras, J. (2012). Microfibrillated cellulose—Its barrier properties and applications in cellulosic materials: A review. *Carbohydrate Polymers, 90*(2), 735–764.

Le Van, H. (2017). Properties of nano-fibrillated cellulose and its length-width ratio determined by a new method. *Cellulose Chemistry and Technology, 51*(7–8), 649–653.

Madani, A., Kiiskinen, H., Olson, J. A., & Martinez, D. M. (2011). Paper physics: Fractionation of microfibrillated cellulose and its effects on tensile index and elongation of paper. *Nordic Pulp & Paper Research Journal, 26*(3), 306–311.

Missoum, K., Bras, J., & Belgacem, M. N. (2012). Water redispersible dried nanofibrillated cellulose by adding sodium chloride. *Biomacromolecules, 13*(12), 4118–4125.

Nair, S. S., Zhu, J. Y., Deng, Y., & Ragauskas, A. J. (2014). High performance green barriers based on nanocellulose. *Sustainable Chemical Processes, 2*(1), 23.

NREL (2005). *NREL TP-510-42619 determination of extractives in biomass: Laboratory Analytical Procedure (LAP) cole boulevard.* Golden, Colorado: National Renewable Energy Laboratory.

Raj, P., Varanasi, S., Batchelor, W., & Garnier, G. (2015). Effect of cationic polyacrylamide on the processing and properties of nanocellulose films. *Journal of Colloid and Interface Science, 447*, 113–119.

Raj, P., Mayahi, A., Lahtinen, P., Varanasi, S., Garnier, G., Martin, D., et al. (2016). Gel point as a measure of cellulose nanofibre quality and feedstock development with mechanical energy. *Cellulose, 23*(5), 3051–3064.

Rowell, R. M. (2012). *Handbook of wood chemistry and wood composites.* CRC Press.

Shanmugam, K., Doosthosseini, H., Varanasi, S., Garnier, G., & Batchelor, W. (2018). Flexible spray coating process for smooth nanocellulose film production. *Cellulose, 25*(3), 1725–1741.

Spence, K. L., Venditti, R. A., Habibi, Y., Rojas, O. J., & Pawlak, J. J. (2010). The effect of chemical composition on microfibrillar cellulose films from wood pulps: Mechanical processing and physical properties. *Bioresource Technology, 101*(15), 5961–5968.

Spence, K. L., Venditti, R. A., Rojas, O. J., Habibi, Y., & Pawlak, J. J. (2010). The effect of chemical composition on microfibrillar cellulose films from wood pulps: Water interactions and physical properties for packaging applications. *Cellulose, 17*(4), 835–848.

Takagi, H., Nakagaito, A. N., & Bistamam, M. S. A. (2013). Extraction of cellulose nanofiber from waste papers and application to reinforcement in biodegradable composites. *Journal of Reinforced Plastics and Composites, 32*(20), 1542–1546.

TAPPI (2002). *T 211 om-02 ash in wood, pulp, paper and paperboard: Combustion at 525 °C.* Technology Park, Atlanta, GA, USA: Technical Association of the Pulp and Paper Industry (TAPPI) Press.

TAPPI (2001a). *T 248 sp-00 laboratory beating of pulp (PFI mill method).* Technology Park, Atlanta, GA, USA: Technical Association of the Pulp and Paper Industry (TAPPI) Press.

TAPPI (2001b). *T 402 sp-98 standard conditioning and testing atmospheres for paper, board, pulp handsheets, and related products.* Technology Park, Atlanta, GA, USA: Technical Association of the Pulp and Paper Industry (TAPPI) Press.

TAPPI (2001c). *T 494 om-96 tensile breaking properties of paper and paperboard (using constant rate of elongation apparatus).* Technology Park, Atlanta, GA, USA: Technical Association of the Pulp and Paper Industry (TAPPI) Press.

Varanasi, S., He, R., & Batchelor, W. (2013). Estimation of cellulose nanofibre aspect ratio from measurements of fibre suspension gel point. *Cellulose, 20*(4), 1885–1896.

Zhang, L., Batchelor, W., Varanasi, S., Tsuzuki, T., & Wang, X. (2012). Effect of cellulose nanofiber dimensions on sheet forming through filtration. *Cellulose, 19*(2), 561–574.

Zimmermann, T., Bordeanu, N., & Strub, E. (2010). Properties of nanofibrillated cellulose from different raw materials and its reinforcement potential. *Carbohydrate Polymers, 79*(4), 1086–1093.